Journal of Power Sources 193 (2009) 841–845

Contents lists available at ScienceDirect

Journal of Power Sources

journal homepage: www.elsevier.com/locate/jpowsour

Short communication

Improved high-rate charge/discharge performances of $LiFePO_4$/C via V-doping

C.S. Sun, Z. Zhou*, Z.G. Xu, D.G. Wang, J.P. Wei, X.K. Bian, J. Yan

Institute of New Energy Material Chemistry, Nankai University, Tianjin 300071, China

ARTICLE INFO

Article history:
Received 19 September 2008
Received in revised form 5 March 2009
Accepted 31 March 2009
Available online 8 April 2009

Keywords:
$LiFePO_4$
Cathode material
Lithium-ion batteries
V-doping

ABSTRACT

V-doped $LiFePO_4$/C cathode materials were prepared through a carbothermal reduction route. The microstructure was characterized by X-ray diffraction, X-ray photoelectron spectroscopy and scanning electron microscopy. The electrochemical Li^+ intercalation performances of V-doped $LiFePO_4$/C were compared with those of undoped one through galvanostatic intermittent titration technique, cyclic voltamperometry, and electrochemical impedance spectrum. V-doped $LiFePO_4$/C showed a high discharge capacity of ~70 mAh g^{-1} at the rate of 20 C (3400 mA g^{-1}) at room temperature. The significantly improved high-rate charge/discharge capacity is attributed to the increase of Li^+ ion "effective" diffusion capability.

1. Introduction

Since Padhi et al. [1] proposed olivine-type $LiMPO_4$ (M = Fe, Co, Mn, or Ni) as cathode materials in Li ion batteries, this kind of compounds have been attracting much research and development interest. Among all these isostructural compounds, $LiFePO_4$, with a theoretical capacity of ~170 mAh g^{-1} and a flat charge/discharge potential at 3.45 V vs. Li^+/Li [1–3], has been established as a promising candidate for next-generation cathode materials in Li ion batteries. $LiFePO_4$ has many advantages over $LiCoO_2$, such as low cost, nontoxic properties, safety advantages, and long cyclic life. Li ion batteries with $LiFePO_4$ as cathode materials also have great potential as power sources for electric vehicles (EV), hybrid electric vehicles (HEV), *etc*.

However, pristine $LiFePO_4$ has the disadvantage of poor rate performances due to its low electrical conductivity (~10^{-9} S cm^{-1}). Considerable efforts have been made to increase its electrical conductivity by carbon coating [4], metal-rich phosphide nanonetworking [5], or super-valence ion doping [6,7]. Through these methods, its electrical conductivity was increased to as high as 4.8×10^{-2} S cm^{-1} [6,8]. Even though, the increased electrical conductivity did not result in the improvement of the rate performances of $LiFePO_4$ as expected. Accordingly the ability of Li^+ ion chemical diffusion in the electrode bulk may play a more important role in the rate capability of $LiFePO_4$.

Recently, other methods have been explored to enhance Li^+ ion diffusion in $LiFePO_4$. Rho et al. [9] proposed that sub-μm or nanoscale $LiFePO_4$ particles minimized the path length for Li^+ transport. Wang et al. [10] reported that the rate capability and cyclic stability of $LiFePO_4$ were greatly enhanced by bivalent cation (Ni, Co or Mg) doping at Fe-site. Under a high rate of 10 C at room temperature, the specific capacity of $LiFe_{0.9}Co_{0.1}PO_4$ maintained at 90.4 mAh g^{-1} [7]. Fe-site doping increased the ionic mobility and diffusion coefficient probably by weakening Li–O interaction. More recently, a composite of $LiFePO_4$ with $Li_3V_2(PO_4)_3$ addition has been prepared [10,11], and both the electrical conductivity and high-rate discharge capacity have been improved, leading to a high discharge capacity of about 100 mAh g^{-1} at 10 C rate. However, this material contained mixed phases of $LiFePO_4$ and $Li_3V_2(PO_4)_3$. So far there has been no report on the electrochemical performances of single-phase vanadium-doped $LiFePO_4$. In this work, V-doped $LiFePO_4$ was prepared, and its structural characteristics and electrochemical Li^+ intercalation performances were investigated.

2. Experimental

2.1. Material preparation

Vanadium-doped $LiFePO_4$/C was prepared via a carbothermal reduction route [12]. The starting materials, containing 0.6895 g $LiNO_3$, 3.9188 g $Fe(NO_3)_3 \cdot 9H_2O$, 0.0351 g NH_4VO_3, 1.1503 g $NH_4H_2PO_4$ and 1.3077 g glucose, were dissolved in distilled water under stirring condition, and then heated at 100 °C. The molar ratio of Li:Fe:V:P in the precursor was 1.05:0.97:0.03:1.00. The resulting precursor was calcined at 350 °C for 4 h and subsequently sintered at 650 °C for 10 h in an argon atmosphere. Carbon converted from glucose acted as reducing and conducting agent and its amount was ~5 wt.% in the final product. The undoped $LiFePO_4$/C sample was

* Corresponding author. Tel.: +86 22 23503623; fax: +86 22 23498941.
E-mail address: zhouzhen@nankai.edu.cn (Z. Zhou).

0378-7753/$ – see front matter © 2009 Elsevier B.V. All rights reserved.
doi:10.1016/j.jpowsour.2009.03.061

also prepared for comparison through the same procedure except the addition of NH_4VO_3.

2.2. Structural and morphological characterization

The crystalline phases of pristine and V-doped $LiFePO_4$/C samples were identified by X-ray diffraction (XRD) under the Rigaku D/MAX III diffractometer with a Cu Kα radiation. For both samples, Rietveld refinement was carried out with the Fullprof program [13]. X-ray photoelectron spectroscopy (XPS) was obtained for the V-doped $LiFePO_4$/C under Kratos Axis Ultra DLD spectrometer with monochromatic Al Kα radiation ($h\nu$ = 1486.6 eV). The morphology was also observed through a Hitachi S-3500N scanning electron microscopy (SEM).

2.3. Electrochemical tests

Test electrodes were prepared as follows. After rolling the mixture of 85 wt.% active materials with 10 wt.% acetylene black and 5 wt.% polytetrafluoroethylene (PTFE) binder, the obtained sheets were cut into circular strips of 8 mm in diameter, and about 5.0 mg cm^{-2} active material was loaded on an Al foil. The strips were dried at 100 °C for 8 h. Electrochemical measurements were conducted in Li test cells with lithium foil as counter and reference electrodes. All the test cells contained 1.0 mol L^{-1} $LiPF_6$ in ethylene carbonate (EC)–ethyl methyl carbonate (EMC)–dimethyl carbonate (DMC) (1:1:1, v/v/v) as electrolyte and were assembled in an argon-filled glove box. Charge/discharge tests were performed between 2.5 and 4.2 V under a Land CT2001 Battery Tester at 20 °C. To get overpotential–composition isotherms, Li insertion/extraction procedures were compared for pristine and V-doped $LiFePO_4$/C by galvanostatic intermittent titration technique (GITT). The series intermittent current was 6×10^{-3} mA for 2.0 h, and then the electrode was left at the open circuit for 2.0 h between each intermittent current regardless of charge or discharge. Cyclic voltammograms (CV) were performed for both pristine and V-doped $LiFePO_4$/C samples at a scanning rate of 50 μV s^{-1}. The electrochemical impedance spectra (EIS) were recorded under the IM6e electrochemical analyzer (ZAHNER-elektrik GmbH & Co. KG, Germany). The frequency range was 10^4–1.0×10^{-2} Hz, and the amplitude was 5 mV. The pristine and V-doped $LiFePO_4$/C pellets used for the electrical conductivity measurements were prepared by uniaxially pressing the active powders with a pressure of 10 MPa, and then Ag paste was coated on both sides of the pellets of about 13 mm in diameter and 1.3 mm in thickness. The electrical conductivity was measured through linear polarization also under the IM6e electrochemical analyzer.

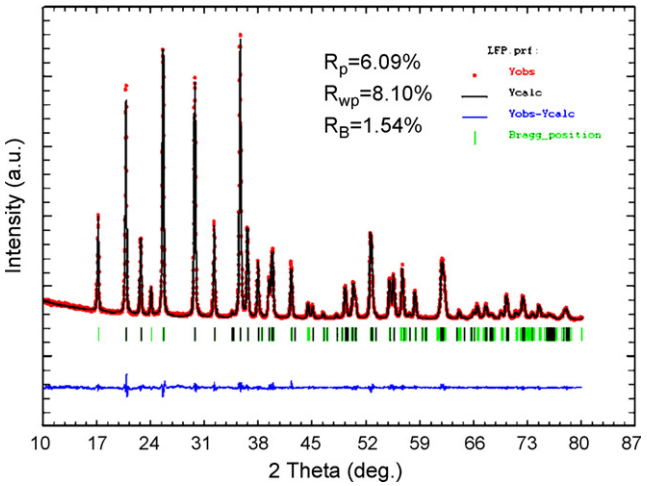

Fig. 1. Rietveld refinement of V-doped $LiFePO_4$ using space group *Pnma*.

Table 1
Lattice constants of pristine and V-doped $LiFePO_4$/C.

	a (Å)	b (Å)	c (Å)	V (Å^3)
$LiFePO_4$/C	10.339	6.014	4.700	292.26
V-doped $LiFePO_4$/C	10.350	6.012	4.704	292.74

3. Results and discussion

3.1. Sample characterization

Pristine and doped $LiFePO_4$/C powders were analyzed by XRD to verify phase purity. The corresponding Rietveld refinement plot of V-doped $LiFePO_4$ is shown in Fig. 1. V-doped $LiFePO_4$ was well crystallized in orthorhombic structure as the pristine one without any unexpected phase. The lattice constants of these two samples are listed in Table 1. V-doping results in slight changes in cell size. The doped one expands the *a*- and *c*-axis by 0.1% and 0.06%, respectively, and shrinks *b*-axis by ca. 0.03%, convincing us that V was introduced into $LiFePO_4$ matrix structure. The cell volume, *V*, of the V-doped $LiFePO_4$ expands about 0.16% compared with that of pristine $LiFePO_4$, which can be attributed to the comparability between the atomic radius of V^{3+} (0.74 Å) and Fe^{2+} (0.74 Å).

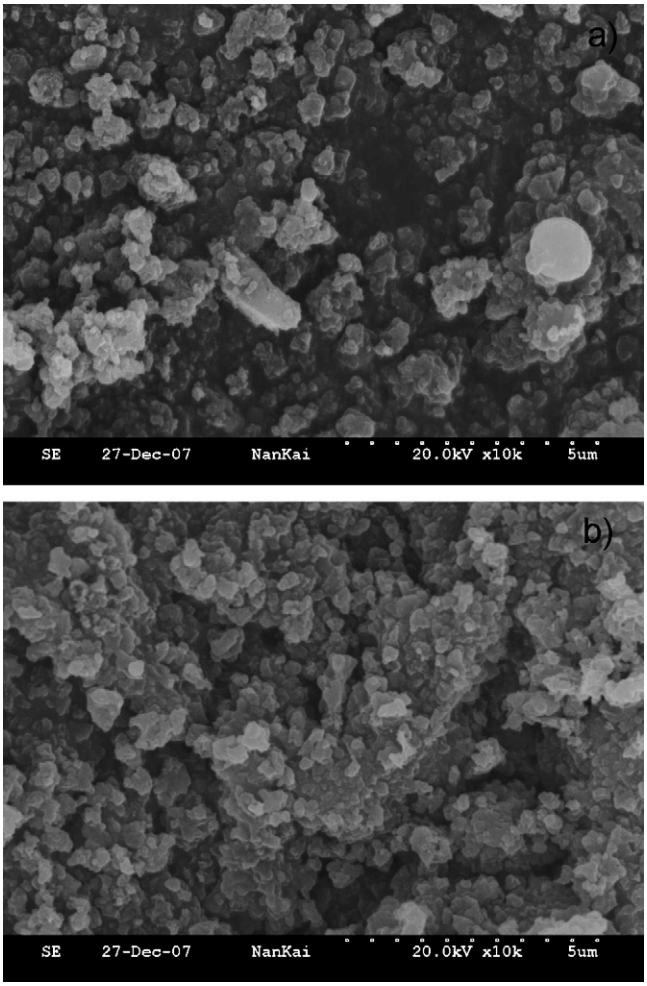

Fig. 2. SEM images of pristine (a) and V-doped $LiFePO_4$/C (b).

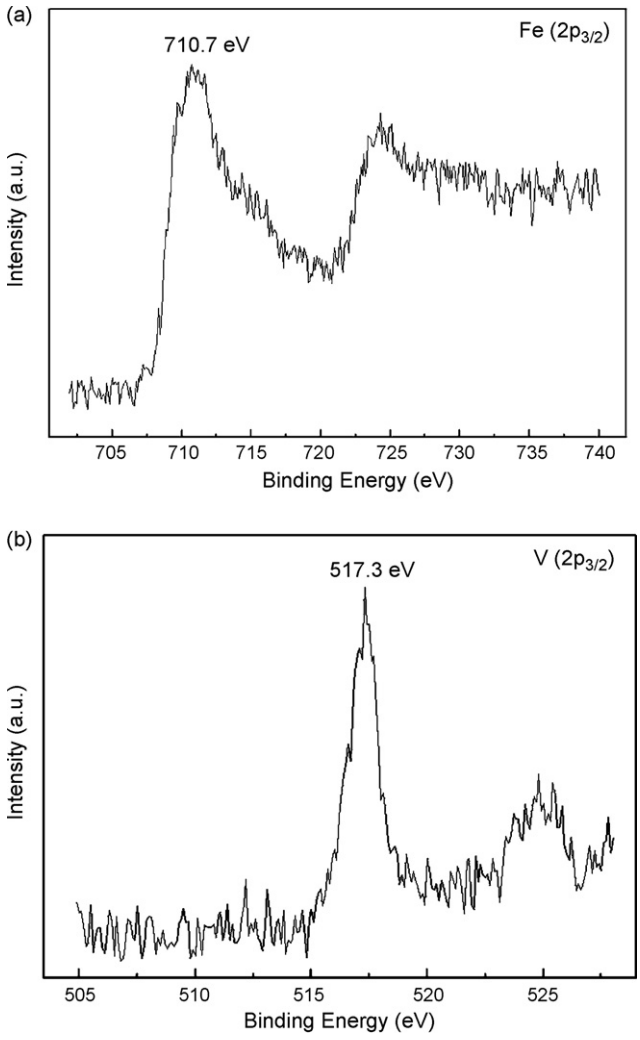

Fig. 3. XPS core levels of Fe($2p_{3/2}$) and V($2p_{3/2}$) in V-doped $LiFePO_4$/C.

Fig. 2 shows the morphologies of pristine and V-doped $LiFePO_4$/C samples. The particle size of pristine $LiFePO_4$/C has a wide distribution range from ~100 nm to more than 1 μm (Fig. 2a), whereas the doped one shows uniform particles (100–200 nm) interconnected with a porous network (Fig. 2b).

The oxidation states of Fe and V were studied by XPS, and the Fe($2p_{3/2}$) and V($2p_{3/2}$) XPS core levels for V-doped $LiFePO_4$ sample are shown in Fig. 3. The Fe($2p_{3/2}$) XPS shows a single peak with a binding energy (BE) of 710.7 eV, indicating that the oxidation state of Fe is +2. The V($2p_{3/2}$) core level fits to a single peak with a BE of 517.3 eV, matching well with that observed in $Li_3V_2(PO_4)_3$ (517.2 eV) [14,15]; therefore, the oxidation state of V in the doped sample is +3. Since the oxidation state of V is higher than that of Fe in the doped $LiFePO_4$, the supervalent doping occurs to olivine $LiFePO_4$. When the supervalent V^{3+} ion is doped in $LiFePO_4$, the charge difference between V^{3+} and Fe^{2+} should be compensated by the M1 site vacancies and the M2 site substitution of Fe^{2+} for Li^+, as in stoichiometric compounds [16].

3.2. Galvanostatic charge/discharge tests

Fig. 4 shows the galvanostatic charge/discharge curves of pristine and V-doped $LiFePO_4$/C cathodes at the first cycle, which were carried out at C/10 (17 mA g^{-1}) between 2.5 and 4.2 V vs. Li^+/Li. V-doped $LiFePO_4$/C exhibits significantly better electrochemical performance with a specific capacity of

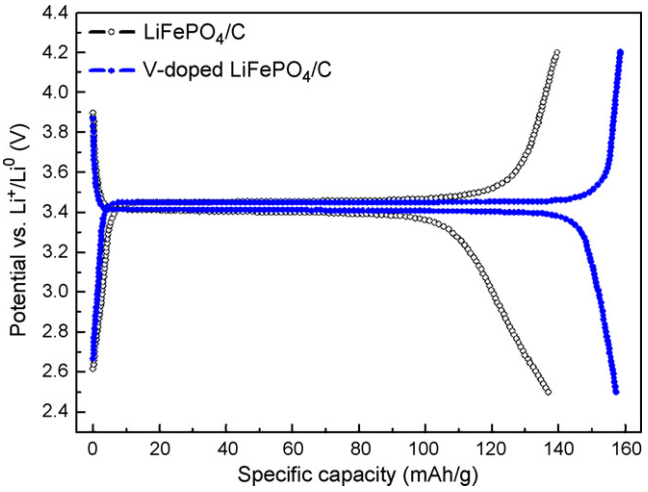

Fig. 4. Charge/discharge curves of the first cycle for pristine and V-doped $LiFePO_4$/C cathodes measured at 0.1 C in the range of 2.5–4.2 V at 20 °C.

168.8 mAh g^{-1}; in contrast, the pristine one presents only ca. 137.5 mAh g^{-1}.

The charge/discharge cycling results of these two samples measured at 20 °C are summarized in Fig. 5. At 10 C rate (1700 mA g^{-1}), V-doped $LiFePO_4$/C shows a specific capacity of about 99.8 mAh g^{-1}, 43 mAh g^{-1} higher than that of the pristine one. At 20 C rate (3400 mA g^{-1}), a capacity of ca. 70 mAh g^{-1} is even obtained for V-doped $LiFePO_4$/C.

To primarily clarify the improvement of $LiFePO_4$ rate performances after V-doping at the electrochemical viewpoint, CV and GITT tests were performed.

3.3. Cyclic voltamperometry (CV)

Fig. 6 shows the CV curves of the pristine and V-doped $LiFePO_4$/C. The CV profile of V-doped $LiFePO_4$ shows sharper shape of the oxidation–reduction peaks than the pristine one does. The details of the polarized potential and the peak current density of the reactions are presented in Table 2, which implies that the peak current densities were enlarged by V-doping, and the reversibility was also improved.

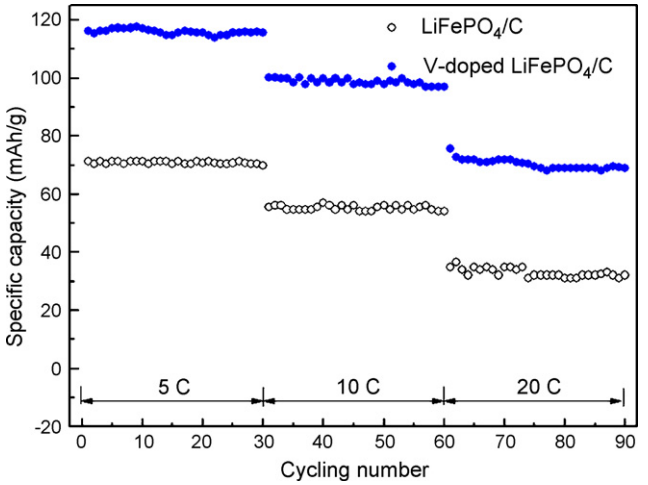

Fig. 5. Cycling performances of pristine and V-doped $LiFePO_4$/C cathodes measured with different rates in the voltage range of 2.5–4.2 V at 20 °C.

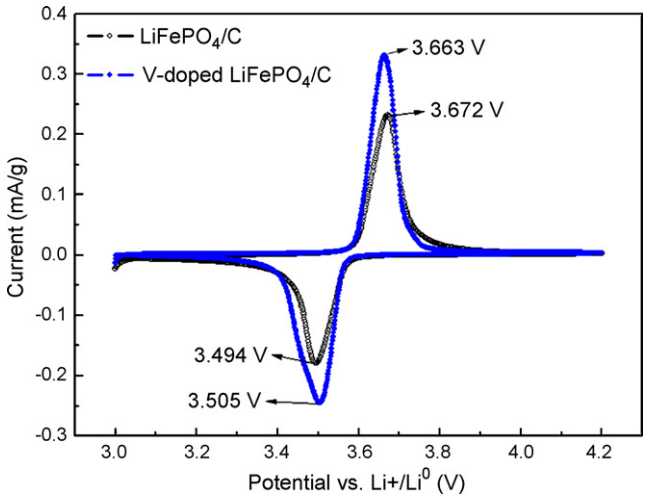

Fig. 6. CV curves of pristine and V-doped $LiFePO_4/C$ measured with a scanning rate of 50 $\mu V\,s^{-1}$ between 3.0 and 4.2 V at 20 °C.

3.4. Li insertion/extraction equilibrium potential–composition isotherm

Fig. 7 shows the GITT charge/discharge curves for the pristine and V-doped $LiFePO_4/C$ measured with a successive current of 6×10^{-3} mA for 2 h followed by a resting time (with open circuit) for 2 h. After the resting time, the open circuit potential for V-doped $LiFePO_4/C$ between charge and discharge is about 12 mV. Noticeably, the breadth of potential fluctuation in the two-phase region increases from 8 mV to more than 40 mV for the pristine one, while it increases from 6 mV to only 16 mV with the increase of Li content in the V-doped $LiFePO_4/C$ cathode.

To sum up, the results of CV and GITT convinced us that the electrochemical reaction of $LiFePO_4$ became more reversible and easier to occur due to the V-doping. Generally, low electrical conductivity and Li^+ ion diffusion in the material bulk are the main factors controlling the high-rate performances of $LiFePO_4$. To clarify the origin of the improved rate capacity, linear polarization and EIS at the fully discharge state were performed to test the electrical conductivity and the Li^+ ion "effective" diffusion coefficient of two materials.

The Li^+ ion "effective" diffusion coefficient for the finite-space solid-state diffusion depends on the Warburg slope of straight line section in Warburg region [17]:

$$A_\omega = \frac{\Delta Re}{(\Delta\omega)^{-1/2}} = \frac{\Delta Im}{(\Delta\omega)^{-1/2}} \quad (1)$$

In Eq. (1), ΔRe and ΔIm are the differences between the real and imaginary components of the ac impedance, respectively, and $\Delta\omega$ is the corresponding finite change in angular frequency.

The EIS plots are presented in Fig. 8 for the V-doped $LiFePO_4/C$ and pristine $LiFePO_4/C$. The Warburg slope can be deduced from Fick's law as follows [18]:

$$A_\omega = \frac{dE/dx}{(\sqrt{2D}FAC_{Li^+})} \quad (2)$$

Table 2
Polarization potential and peak current density of pristine and V-doped $LiFePO_4/C$ cathodes.

	E_{Ox} (V)	E_{Red} (V)	$\Delta E_{(Ox-Red)}$ (V)	i_p (Ox) ($mA\,g^{-1}$)	i_p (Red) ($mA\,g^{-1}$)
V-doped $LiFePO_4/C$	3.663	3.505	0.158	0.331	0.245
$LiFePO_4/C$	3.672	3.494	0.178	0.232	0.179

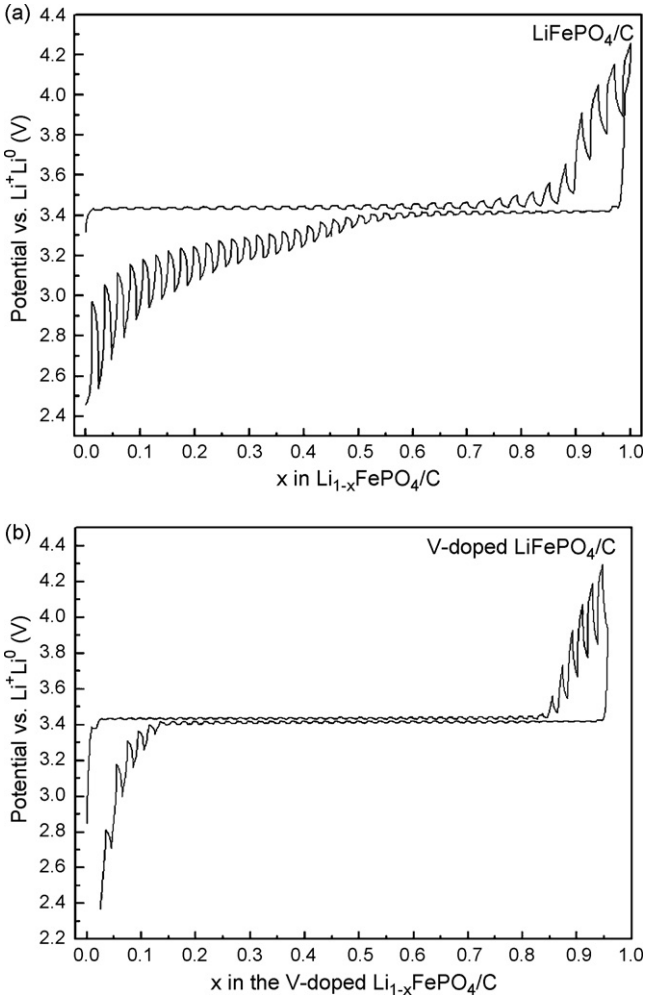

Fig. 7. Galvanostatic intermittent charge/discharge curves for pristine $LiFePO_4/C$ (a) and V-doped $LiFePO_4/C$ (b) measured at 20 °C with a successive current of 6×10^{-3} mA for 2 h followed by a resting time (with open circuit) for 2 h.

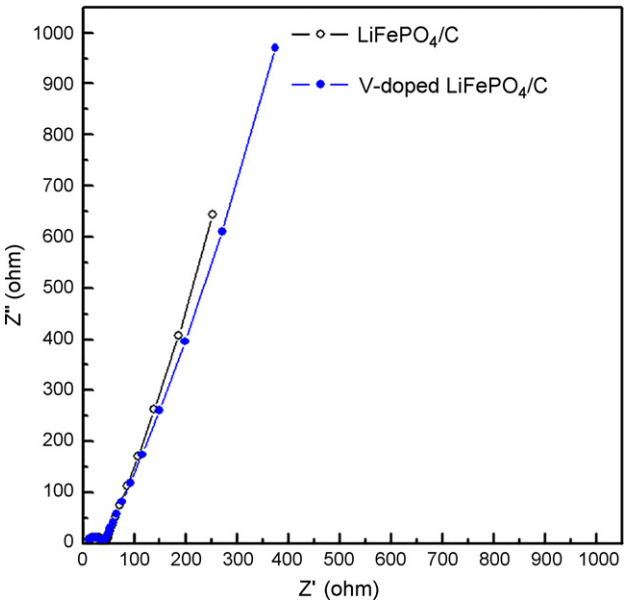

Fig. 8. Impedance responses of V-doped $LiFePO_4/C$ and $LiFePO_4/C$ measured at the fully discharged state at 25 °C.

Table 3
Electrical conductivity and Li^+ ion diffusion coefficient of pristine and V-doped $LiFePO_4/C$.

	$LiFePO_4/C$	V-doped $LiFePO_4/C$
Electrical conductivity ($S\,cm^{-1}$)	8.49×10^{-3}	4.57×10^{-4}
Li^+ ion diffusion coefficient ($cm^2\,s^{-1}$)	2.90×10^{-11}	1.86×10^{-10}

where A is the surface area in cm^2 of the electrode, D, the chemical diffusion coefficient ($cm^2\,s^{-1}$), F, the Faraday constant, C_{Li^+}, the bulk concentration of Li^+ in electrode ($0.0228\,mol\,cm^{-3}$), and dE/dx is the slope of the electrode potential (E) vs. x in Li_xFePO_4. To get the exact value of dE/dx, the ac impedance should be carried out at the potential of lower or higher than the plane potential where the value of dE/dx is almost zero and hence irresponsible. Here, we obtained D at the fully discharged state.

The electrical conductivity and Li^+ ion "effective" diffusion coefficient are listed in Table 3 for the pristine and V-doped $LiFePO_4/C$. It is known that the electrical conductivity in the olivine $LiFePO_4$ is $\sim 10^{-9}\,S\,cm^{-1}$, and the Li^+ ion "effective" diffusion coefficient is found to be $\sim 10^{-14}\,cm^2\,s^{-1}$ [19]. As for our results in Table 3, the electrical conductivity of the materials was improved to 10^{-3}–$10^{-4}\,S\,cm^{-1}$ by the existence of carbon, while the electrical conductivity of pristine $LiFePO_4/C$ was greater than that of the doped one. The uniformly distributed smaller particles and V^{3+}-doping in the lattice of $LiFePO_4$ may both affect the electrical conductivity of the materials. On the other hand, the Li^+ ion "effective" diffusion coefficient of the V-doped $LiFePO_4/C$ was improved to $1.86 \times 10^{-10}\,cm^2\,s^{-1}$, about one order of magnitude higher than that of the pristine one. The results in Table 3 suggest that, although the electrical conductivity was improved to the level of $\sim 10^{-3}\,S\,cm^{-1}$, the increased electrical conductivity did not result in better rate performances of the pristine $LiFePO_4/C$ as expected. Therefore, it is believed that the Li^+ "effective" ionic diffusion plays a more important role of the improved rate performances of V-doped $LiFePO_4/C$. When the electrical conductivity is as high as $10^{-3}\,S\,cm^{-1}$, the kinetic characteristics of the electrochemical reactions are dominated by Li^+ ion diffusion.

The improvement of Li^+ ion diffusion in the V-doped $LiFePO_4$ can partly be attributed to the optimization of the microstructure. SEM images show that the particle size becomes more uniform after the V-doping. The uniformly distributed particles with smaller sizes tend to offset the barrier to high rates governed by the sluggish charge transport of phosphates [3]. On the other hand, Li^+ ions transport along c-axis with lower diffusion energy barrier [20], since super-valence doping may induce microstructure distortion. To get the mircostructural information, Rietveld refinement of XRD was conducted and the results are disclosed in Table 1. V-doping expands the a- and c-axis, and Li^+ ion transportation may be facilitated for V-doped $LiFePO_4$. Totally, the optimization of the Li^+ ion diffusion in the V-doped $LiFePO_4/C$ can be attributed both to the uniform distribution of the minimized particles and to the super-valence doping.

4. Conclusion

Well crystallized powders of V-doped $LiFePO_4/C$ with uniformly distributed particles were prepared via the carbothermal reduction route and investigated using XRD, XPS, SEM, GITT, CV and EIS. The V-doped $LiFePO_4/C$ presented a higher rate capability than the pristine one did. This can be attributed to the optimization of the morphology and the crystal microstructure, which facilitates the Li^+ ion diffusion. Therefore, it is an effective way to optimizing the rate performances of $LiFePO_4/C$ by the V-doping on the basis of the improvement of electrical conductivity.

Acknowledgements

This work was supported by the 863 Program (2007AA03Z225), the 973 Program (2009CB220100), and Tianjin NSF (06YFJMJC13300) in China.

References

[1] A.K. Padhi, K.S. Nanjundaswamy, J.B. Goodenough, J. Electrochem. Soc. 144 (1997) 1188.
[2] N. Terada, T. Yanagi, S. Arai, M. Yoshikawa, K. Ohta, N. Nakajima, N. Arai, J. Power Sources 1–2 (2001) 80.
[3] A. Yamada, S.C. Chung, K. Hinokuma, J. Electrochem. Soc. 148 (2001) A224.
[4] M.M. Doeff, Y. Hu, F. Mclarnon, R. Kostecki, Electrochem, Solid State Lett. 6 (2003) A207.
[5] P.S. Herle, B. Ellis, N. Coombs, L.F. Nazar, Nat. Mater. 3 (2004) 147.
[6] S.Y. Chung, J.T. Bloking, Y.M. Ching, Nat. Mater. 1 (2002) 123.
[7] D.Y. Wang, H. Li, S.Q. Shi, X.J. Huang, L.Q. Chen, Electrochim. Acta 50 (2005) 2955.
[8] S.Y. Chung, Y.M. Chiang, Electrochem, Solid State Lett. 6 (2003) A278.
[9] Y.H. Rho, L.F. Nazar, L. Perry, D. Ryan, J. Electrochem. Soc. 154 (2007) A283.
[10] L.N. Wang, Z.C. Li, H.J. Xu, K.L. Zhang, J. Phys. Chem. C 112 (2008) 308.
[11] D. Choi, P.N. Kumta, J. Power Sources 163 (2007) 1064.
[12] R.K.B. Gover, A. Bryan, P. Burns, J. Barker, Solid State Ionics 177 (2006) 1495.
[13] J. Rodrrguez-Carvajal, Physica B 192 (1993) 55.
[14] M.M. Ren, Z. Zhou, Y.Z. Li, X.P. Gao, J. Yan, J. Power Sources 162 (2006) 1357.
[15] Y.Z. Li, Z. Zhou, M.M. Ren, X.P. Gao, J. Yan, Electrochim. Acta 51 (2006) 6498.
[16] M. Wagemaker, B.L. Ellis, D. Lützenkirchen-Hecht, F.M. Mulder, L.F. Nazar, Chem. Mater. 20 (2008) 6313.
[17] S.B. Tang, M.O. Lai, L. Lu, J. Alloys Compd. 449 (2008) 300.
[18] C. Ho, I.D. Raistrick, R.A. Huggins, J. Electrochem. Soc. 127 (1980) 343.
[19] P.P. Prosini, M. Lisi, D. Zane, M. Pasquali, Solid State Ionics 148 (2002) 45.
[20] M.R. Yang, W.H. Ke, S.H. Wu, J. Power Sources 146 (2005) 539.